THE JOURNAL OF PHYSICAL CHEMISTRY A

pubs.acs.org/JPCA Article

Description of Two-Particle One-Hole Electronic Resonances Using Orbital Stabilization Methods

Mushir Thodika, Nathan Mackouse, and Spiridoula Matsika*

Cite This: https://dx.doi.org/10.1021/acs.jpca.0c07904 Read Online

ACCESS | Metrics & More | Article Recommendations | Supporting Information

ABSTRACT: Two-particle one-hole (2p-1h) resonances are elusive to accurate characterization, their decay to the neutral state being a two-electron process. Although in limited cases, single reference methods can be used, a proper description of a 2p-1h resonant state entails a multiconfigurational treatment of the reference wavefunction. In this work, we test the performance of the orbital stabilization method to characterize the 2p-1h resonances found in water and benzene. We employ a set of two multireference approaches, namely, the restricted active space self-consistent field and the multireference configuration interaction, as well as the single reference method equation of motion for electron attachment coupled-cluster with singles and doubles, in the case of benzene. We further explore the resonant channel mixing in benzene between the B_{2g} shape resonance and 2p-1h resonance, a phenomenon which has been explored quite often in experimental studies.

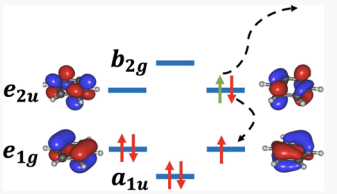

INTRODUCTION

Temporary anion resonances have captivated the curiosity of both experimentalists and theorists alike, because of their prevalence in a myriad of chemical and biological processes, and the underlying challenges accompanying the accurate characterization of these transient species. These metastable anions, otherwise known as electronic resonances, are formed as intermediates in low-energy ($E \leq 20$ eV) electron-induced processes occurring in a variety of environments. A detailed understanding of low-energy electron-induced reactions has several implications in astrochemistry, condensed-phase processes, and radiation damage to living cells and others.[1−7] Resonances are broadly categorized into shape or core-excited resonances depending on the electronic configuration of the neutral target preceding the electron attachment. In the molecular orbital picture, a shape resonance (or a single particle resonance) is formed when the incoming electron is captured into one of the unoccupied valence orbitals of the neutral molecule. The name "shape" refers to the centrifugal barrier formed in the electron−molecule interaction potential which traps the incoming particle momentarily. Shape resonances are generally short-lived with lifetimes ranging from femtoseconds to few hundreds of picoseconds.[8] Alternatively, the incoming electron can induce an excitation in the neutral target and thereby attach itself to an excited state of the parent system. The anionic states thus formed are commonly known as core-excited or two-particle-one-hole (2p-1h) resonances, which are found at higher energies relative to shape resonances. It should be noted that core-excited resonances are not related to core electrons, but here we adopt the terminology used by the scattering theory community. The decay of core-excited resonances is a two-electron process, and thus they are associated with longer lifetimes. Depending on the relative energy of the core-excited resonance with respect to the parent excited state, they can be further classified into either "core-excited shape" (when the resonance is unstable with respect to the neutral excited state) or "Feshbach" (when it is stable with respect to the neutral excited state) type. Figure 1 demonstrates these two different types of resonances,

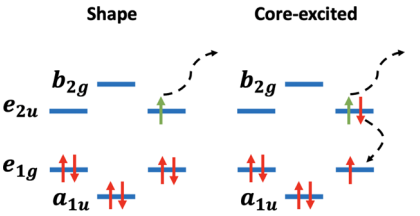

Figure 1. Shape and 2p-1h resonances in benzene.

as seen in benzene. The shape resonance is formed by attachment to a π^* orbital, while the core-excited resonance involves an excitation $\pi \rightarrow \pi^*$ and attachment to the π^* orbital.

Transient anions do not satisfy the boundary conditions required for conventional bound-state methods and are consequently difficult to characterize using standard quantum chemistry packages.[9] In the time-dependent picture, a transient state is represented by a manifold of states in the continuum eigenspectrum of a Hermitian Hamiltonian, which makes it

Received: August 30, 2020
Revised: October 6, 2020

non-L^2 integrable.[10] Hermitian methods can be made to converge to a metastable state with a small basis set, but it might not be the correct one as there are multitudes of states in the vicinity of the actual resonance.[9] On the other hand, using highly diffuse basis functions to describe the metastable state leads to variational collapse of the wavefunction to a neutral parent and a free electron. Resonant states have significant probability inside the interaction region which decays as a function of time, and this can be represented in terms of complex energies (also known as Siegert energies)[11,12]

$$E_{res} = E_R - i\frac{\Gamma}{2} \tag{1}$$

where "E_R" is the position of the resonance and "Γ" is the width of the resonance (the inverse of which provides the lifetime). To retrieve the complex energies associated with metastable states, we need to modify the existing methods to yield complex eigenvalues. This can be done by analytically continuing either the eigenvalues (in case of stabilization methods) or the matrix elements of the Hamiltonian (in case of non-Hermitian quantum mechanics) into the complex plane.[13,14] The former set of methods does not require any modifications to the existing bound-state techniques, whereas the latter family of methods requires significant modifications to conventional methodologies. Stabilization and non-Hermitian methods have been employed frequently over time to investigate shape and core-excited resonances in a variety of molecular systems.[12,14−22] Recently, our study comparing stabilization and complex absorbing potential (CAP)-based methods for shape resonances in small- to medium-sized systems has shown that the performance of both methods is similar in accuracy.[23] Despite the heavy computational cost, CAP-based methods, such as the CAP-equation of motion coupled-cluster (EOM-CC) approach, which is a type of non-Hermitian method, offer a more general and rigorous approach for electronic resonances. These methods have also been recently extended to include computation of analytic gradients, molecular properties, and exceptional points.[24−28] Stabilization methods, however, have the obvious advantage of being computationally inexpensive as they utilize state-of-the-art electronic structure codes developed for bound states. It is worth mentioning that stabilization methods also find use in the calculation of potential energy surfaces of anionic resonances and complex transition dipoles between the resonance states.[29−31]

In this study, we are focusing on the description of core-excited, or 2p-1h, resonances. We are using the stabilization method to study a Feshbach core-excited resonance in water and a shape and core-excited resonance in benzene, using them as benchmark systems since they have been studied extensively in the past. Benzene provides the opportunity to investigate the mixing of resonant channels as well, which is present in many organic conjugated molecules, and requires multireference methods in order to describe this coupling.

METHODS

Orbital Stabilization Method. The stabilization method, first developed by Hazi and Taylor, extrapolates the use of Hermitian methods beyond bound states.[32] Stabilization is incredibly powerful in the sense that it circumvents the need to modify existing computational techniques and makes use of highly efficient codes developed for bound states. The basic idea behind the stabilization approach is to encapsulate the resonant state in an artificial box potential where the energy of the resonance is then monitored with the variation in the box size. In the orbital stabilization method (OSM), the spatial extent of the most diffuse Gaussian functions acts as the confining potential, and the box size is varied by changing the exponent of these Gaussian functions with a scaling parameter (α). The resonances are identified as stable states in the stabilization plots, exhibiting avoided crossings with pseudo-continuum states. The eigenvalues involved in the avoided crossings are analytically continued to the complex plane to obtain the Siegert energy associated with a given resonant state.[21,22,33,34] The analytical continuation is performed by means of generalized Padé approximants (GPAs).[35] The GPA used in this work is given by a quadratic polynomial

$$E^2P + EQ + R = 0 \tag{2}$$

The P, Q, and R coefficients in the GPA expansion are polynomials of the scaling parameter (α)

$$P = 1 + \sum_{i=1}^{n_i} p_i\alpha^i \qquad Q = \sum_{j=0}^{n_j} q_j\alpha^j \qquad R = \sum_{k=0}^{n_k} r_k\alpha^k \tag{3}$$

Equation 2 can be referred to as the (n_i, n_j, n_k) GPAs. The indices corresponding to the expansions of the P, Q, and R coefficients are held equivalent, and the total number of unknowns in the expansion is given by the sum ($n_i + n_j + n_k + 2$). These unknowns are found by a set of linear equations via the standard matrix method. The stationary points, α^*, then are computed according to eq 4[21,36]

$$\frac{dE}{d\alpha} = 0 \tag{4}$$

The computed α^* is then substituted back into eq 2 to retrieve the complex energies.

Electronic Structure. *Water.* The geometry of water was optimized at the MP2 level of theory with augmented-correlation-consistent triple valence zeta (aug-cc-pVTZ) basis set. For stabilization calculations on the water anion, the restricted active space self-consistent field (RASSCF) method and the multireference configuration interaction with singles and doubles (MR-CISD) were employed. Highly diffuse basis sets are required for studying anions to efficiently describe the extra electron which is either loosely bound or is unbound with a finite lifetime, in the case of resonances. In this study on water, we augment the parent basis aug-cc-pVTZ with an additional set of "3s," "3p," and "3d" functions on the oxygen atom. The parent basis is left unmodified on the hydrogens. The exponents for the extra set of diffuse functions were obtained in an even-tempered manner ($\alpha_{i+1} = 0.5 \times \alpha_i$). A summary of the orbitals included in the active space in the restricted active space (RAS) calculation is provided in Table 1

Table 1. Orbital Occupation Table for the Calculation of $^2B_1$ Feshbach Resonance in Water at RASSCF/aug-cc-pVTZ +[3s3p3d] Level of Theory

C_{2v}	CLOSED	ACT	AUX
A_1	2	2	0
B_1	0	1	9
B_2	0	2	0
A_2	0	0	0

https://dx.doi.org/10.1021/acs.jpca.0c07904
J. Phys. Chem. A XXXX, XXX, XXX−XXX

and Figure S1 in the Supporting Information, while Figure 2 shows the molecular orbital diagram with the C_{2v} symmetry

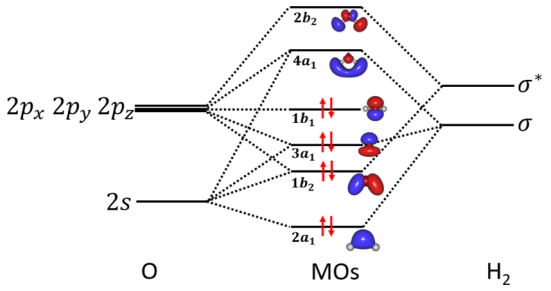

Figure 2. Molecular orbital diagram of neutral water molecule. Symmetry labels are given according to the C_{2v} point group.

labels. The 1s and 2s on O are doubly occupied, while the valence orbitals (2p on O and 1s on H) are included in the active space (ACT) and the diffuse orbitals with symmetry corresponding to that of the Feshbach resonance are included in the auxiliary space (AUX). Both single and double excitations into the AUX space are considered. The energies of the excited states are obtained by state-averaging over the first 15 states. The neutral reference is also calculated at the RASSCF level by state-averaging over the same number of states. MR-CISD calculations on the water anion and the neutral ground state were carried using the same RAS mentioned in Table 1.

Benzene. The ground-state equilibrium structure of benzene was obtained at the B3LYP level of theory with Dunning's cc-pVTZ basis set.[37] Stabilization calculations were carried out at the equation of motion-electron attachment-coupled-cluster singles and doubles (EOM-EA-CCSD) methodology[38−41] and at the multireference level with RASSCF and MR-CISD. The internally contracted MRCI algorithm[42] in MOLPRO was used to do the computation of excited states. The basis set used for the stabilization calculations was cc-pVTZ with an additional "p" function obtained in an even-tempered manner added on carbon atoms. The same basis set was also used to calculate singlet and triplet excited states of neutral benzene using equation of motion for electronically excited states coupled-cluster singles and doubles (EOM-EE-CCSD).

In the RAS calculation, all valence π orbitals [$1b_{1u}$ (a_{2u}), $1b_{2g}$ + $1b_{3g}$ (e_{1g}), $2b_{1u}$ + $1a_u$ (e_{2u}), and $2b_{2g}$ (b_{2g}) in the D_{2h} representation (and D_{6h} in parenthesis)] were included in the main ACT. Figure 3 shows the molecular orbital diagram with the symmetry labels. An additional set of two diffuse orbitals corresponding to the symmetry of the core-excited resonance (B_{2g}) were added to the AUX space. Final set of active and auxiliary orbitals are shown in Figure S2. Calculations were

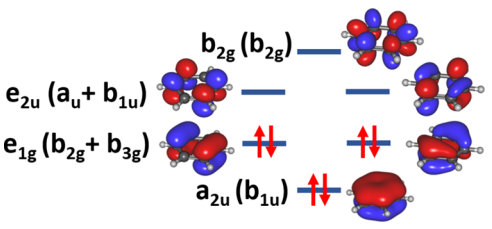

Figure 3. π-orbitals of neutral benzene. Symmetry labels are given according to D_{6h} and the highest Abelian point group of benzene, D_{2h} (in parenthesis).

done in the D_{2h} point group, and B_{2g} states were calculated (which are B_{2g} or E_{1g} in D_{6h}). The state-averaging was done over the first six excited states. The MR-CISD calculation was performed using the same RAS with both single and double excitations into the virtual space.

In addition to the stabilization calculations, low-level complete active space self-consistent field (CASSCF) calculations were also performed in order to obtain a qualitative description of the resonances and their ordering. In these calculations, the cc-pVDZ basis set was used and a (7,6) ACT.

All geometry optimizations for water and benzene were done using Gaussian 09,[43] while RASSCF and MR-CISD calculations were carried out using the MOLPRO suite of programs.[44] EOM-EA-CCSD and EOM-EE-CCSD calculations were performed using the QChem electronic structure program.[45]

RESULTS AND DISCUSSION

Water Feshbach Resonances. The electronic configuration of water in the C_{2v} symmetry is shown in Figure 2. The $1a_1$ and $2a_1$ are mostly 1s and 2s orbitals of O, while the $1b_2$ and $3a_1$ are bonding with H. $1b_1$ is nonbonding, corresponding to the out-of-plane lone-pair orbital of O. The first unoccupied orbital, $4a_1$, is the antibonding counterpart to the $3a_1$ orbital. The lowest electronic excited states of water are formed by excitation of an electron from one of the $1b_1$, $3a_1$, or $1b_2$ orbitals to the $4a_1$ orbital, leading to singlet and triplet states, $^{1,3}B_1$, $^{1,3}A_1$, and $^{1,3}B_2$. The lowest core-excited resonance is formed by attachment of an electron to the $4a_1$ orbital in the $^3B_1$ state, leading to the $^2B_1$ resonance. The nature of this particular excitation has been a source of contention between researchers. In a theoretical study conducted by Rubio et al. at MS-CASPT2 level of theory, the computed $\langle r^2 \rangle$ for the $^3B_1$ state stood at 27.5 a.u., indicating the highly diffuse nature of the excited orbital.[46] Even though the orbital is diffuse enough to not be considered as a valence state, it is also not diffuse enough to be a pure Rydberg state. They conclude that the excited orbital is of an intermediate type and the triplet state undergoes molecular orbital Rydbergization, a phrase termed to suggest the valence-Rydberg mixing by Mulliken.[47] The energy of the resonance is lower than the parent excited state, and it is therefore classified as "Feshbach" resonance. The $^2B_1$ resonance is narrow and lies energetically close to its parent $^3B_1$ state.

Experimental studies on the dissociative electron attachment of water anion has shown that the reaction proceeds through metastable intermediates in the form of three Feshbach resonances. The $^2B_1$ resonance is experimentally known to have a position of 6.5 eV.[48−51] In this study, we investigate this lowest core-excited resonance in the water anion. Extensive previous theoretical and experimental work on the resonances of water makes it a suitable candidate for our study. As a narrow resonance, it provides a contrast to the shape resonance, which will be discussed later.

Here, we have attempted to characterize the Feshbach resonance in water using the stabilization method with multireference theory. It should be pointed out that we also tried to calculate the resonance using the EOM-EA-CCSD method by starting from a triplet reference, but the lowest triplet reference obtained from Unrestricted Hartree Fock (UHF) did not correspond to the parent $^3B_1$ state, so the reference obtained at CCSD was incorrect.

https://dx.doi.org/10.1021/acs.jpca.0c07904
J. Phys. Chem. A XXXX, XXX, XXX−XXX

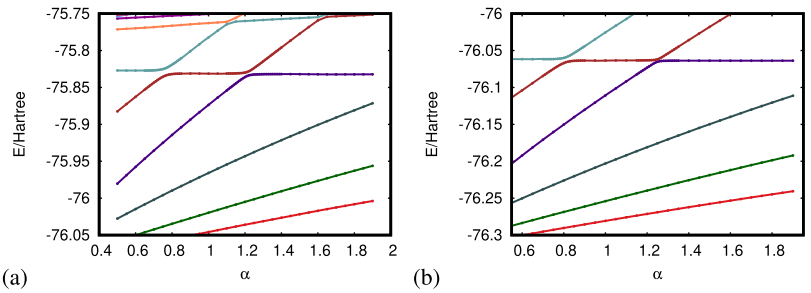

Figure 4. Stabilization curves of $^2B_1$ Feshbach resonance in water at (a) RASSCF/aug-cc-pVTZ+[3s3p3d] and (b) MR-CISD/aug-cc-pVTZ +[3s3p3d] levels of theory.

Multireference Results. The stabilization curves at the RASSCF level are shown in Figure 4a. Two well-defined avoided crossings are obtained. Analytic continuation results for the avoided crossings corresponding to the $^2B_1$ Feshbach resonance in water anion are summarized in Table 2. The positions of the resonances are reported in eV relative to the ground state of the neutral, calculated at the same level of theory.

Table 2. Resonance Positions and Widths in eV Obtained at the RASSCF and MR-CISD Levels for the $^2B_1$ Feshbach Resonance in Water[a]

	$E_R(\Gamma)$	
GPA	AC1	AC2
	RASSCF	
(3,3,3)	6.69 (0.000)	N/A
(4,4,4)	6.69 (0.000)	6.69 (0.003)
(5,5,5)	6.70 (0.000)	6.69 (0.006)
	MR-CISD	
(3,3,3)	7.25 (0.000)	7.19 (0.006)
(4,4,4)	7.24 (0.006)	7.20 (0.007)
(5,5,5)	7.25 (0.008)	7.20 (0.007)

[a]The resonance stabilization curves have two avoided crossings (AC1 and AC2) in both cases that are analyzed.

The position from the first and second avoided crossings stands at 6.69 eV and is consistent at all GPAs and both avoided crossings. However, the widths obtained from the avoided crossings are different from each other. Since the imaginary component of the stationary point from the analytical continuation on the first avoided crossing was zero, we were not able to extract any information regarding the width. From the second avoided crossing however, we obtain a finite width of 0.003 eV at (4,4,4) expansion of the GPA and 0.006 eV at (5,5,5) expansion.

We also computed the resonance parameters for the $^2B_1$ state at the MR-CISD level, which once again manifests itself in the form of two avoided crossings in the stabilization plot (Figure 4b). The analytical continuation results for the avoided crossings are reported in Table 2. From the first avoided crossing, we get a position of 7.25 eV, which is consistent across all expansions of the GPA and a finite width of 0.006 and 0.008 eV at (4,4,4) and (5,5,5) expansions of the GPA, respectively. The analysis of the second avoided crossing reveals a position of 7.20 eV, consistent with all expansions of the GPA. The width changes when we move from (3,3,3) to (4,4,4) expansion but remains consistent across the higher-order expansions.

Comparison with Previous Results. Extensive theoretical studies over the last two decades have investigated the formation of Feshbach resonances in water and their dynamics leading to dissociative attachment processes. A summary of the previous theoretical and experimental results is reported in Table 3. Experimental estimates place the position of the $^2B_1$ Feshbach resonance at 6.5 eV, as seen in Table 3. The position determined at the RASSCF level is close to this value, while that from MR-CISD is approximately 0.7 eV higher. There are no experimental values for the width, but there are theoretical values based on the scattering theory.[52−54] The most recent calculations by Haxton et al. investigated the complex potential energy surfaces of the water anion using complex Kohn variational calculations and reported a width of 6.0−10 meV for the $^2B_1$ Feshbach resonance. Our values at the MR-CISD level are within this range, while the RASSCF values are somewhat smaller. Given the very small value of the widths, this is a very good agreement.

Table 3. Selected Previous Experimental and Theoretical Studies on the Dissociative Attachment in Water Anion Are Listed along with the Position of the $^2B_1$ Feshbach Resonance[a]

	$E_R(\Gamma)$
Lozier[48] (exp)	6.6
Mann et al.[49] (exp)	7.1 ± 0.5
Buchelnikova[55] (exp)	6.4
Schulz[50] (exp)	6.5 ± 0.1
Compton and Christophorou[51] (exp)	6.5 ± 0.1
Trajmar and Hall[56] (exp)	6.5
Jungen et al.[57] (exp)	7.0
Belic et al.[58]	6.5
Gorfinkiel et al.[52] (theory)	6.99 (0.004)
Haxton et al.[54] (theory)	6.09 (0.010)

[a]The value in the brackets indicates the width of the resonance. Positions and widths are given in eV.

An important uncertainty in our calculations is how we compute the ground-state reference. Some uncertainties in the calculated positions are expected because of differences in electron correlation arising from the state-averaging over multiple excited states. In the RAS study on water anion, state-averaging over 15 states was done to determine the energies of the excited states and the ground state. The sensitivity in the resonance positions due to state-averaging of the ground-state energy is shown by comparing the results between averaging 15 states or just 1 state. The energy is overestimated by more than 2 eV at the RASSCF level, when no averaging is used in the neutral, but only by 0.25 eV at the MR-CISD level.

https://dx.doi.org/10.1021/acs.jpca.0c07904
J. Phys. Chem. A XXXX, XXX, XXX−XXX

Including higher-order excitations into virtual space and increasing the size of the basis set could improve the calculated energies. Nevertheless, stabilization method coupled with multireference calculations yield satisfactory results for the resonance parameters when compared to the experiment.

Benzene Resonances. Figure 3 shows the valence orbitals in benzene. The shape resonances in benzene originate from attachment of an electron to the unoccupied π^* (e_{2u} and b_{2g}) orbitals. The resulting ground state in the anion has $^2E_{2u}$ symmetry and is subject to the Jahn−Teller effect.[59] The next shape resonance has $^2B_{2g}$ symmetry. The core-excited states originate from attachment to an excited state of benzene. The lowest excited states in benzene calculated using EOM-EE-CCSD are shown in Figure 5. The lowest states are between 4

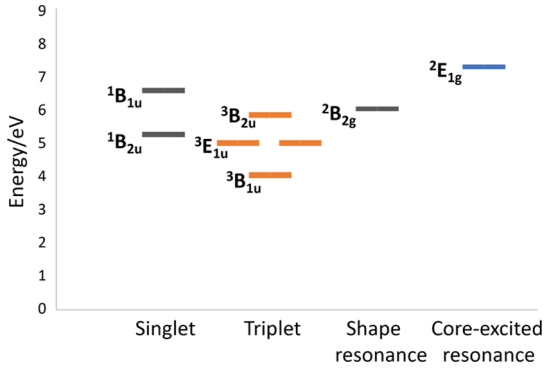

Figure 5. Energy level diagram of the neutral and anion states in benzene calculated at the EOM-EE-CCSD and EOM-EA-CCSD levels, respectively.

and 6 eV, and they are triplet states originating from $\pi \rightarrow \pi^*$ ($e_{1g} \rightarrow e_{2u}$ in D_{6h} symmetry) excitations, $^3B_{1u}$, $^3E_{1u}$, and $^3B_{2u}$.[60−64] The first singlet state $^1B_{2u}$ is also in this energy range, while the other singlet states are higher in energy. Attachment of an electron to the e_{2u} lowest unoccupied molecular orbital (LUMO) of the $^3B_{1u}$ state will lead to a E_{1g} resonance, while attachment to the $^3E_{1u}$ state leads to resonances B_{1g}, B_{2g}, and E_{1g}, and finally, attachment to the higher $^3B_{2u}$ leads to another E_{1g} resonance. The lowest core-excited resonances then are expected to have E_{1g} (three of them) and B_{1g}, B_{2g} symmetries. Electron transmission spectra show that there are a number of resonances near 5.7 and 7.5 eV which are likely corresponding to these five core-excited resonances.[65−67] The B_{2g} core-excited resonance can mix with the B_{2g} shape resonance. Furthermore, the E_{1g} resonances are subject to the dynamical Jahn−Teller effect.[68] In lowering the symmetry to the D_{2h} group, this state splits into $B_{2g} + B_{3g}$, and the B_{2g} components can further mix with the B_{2g} shape resonance. Mixing of the B_{2g} shape resonance with all these core-excited resonances can explain the experimental observation that the resonance can decay to all triplet states.[65,66,69] In this work, we want to explore the B_{2g} shape resonance and the low lying core-excited resonances and their possible mixing.

Low-level CASSCF calculations with a cc-pVDZ basis set and a (7,6) CAS were used to obtain a qualitative description of the resonances and their ordering. Figure 6 shows the states of the anion in D_{6h} symmetry, while on the right, the splitting of the states in D_{2h} symmetry is shown. The lowest $^2E_{2u}$ shape resonance splits into ^2A_u and $^2B_{1u}$, while the next one is the $^2B_{2g}$ shape resonance of interest in this work. The next states are core-excited resonances. The lowest two have E_{1g}

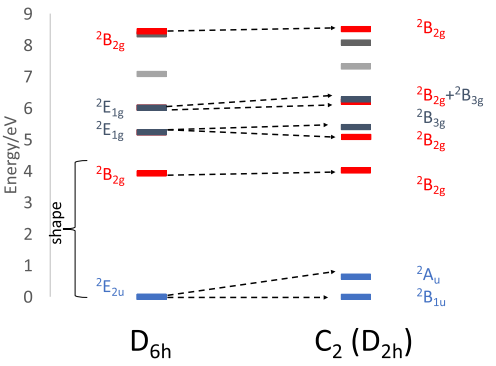

Figure 6. Energy level diagram of the anion states in benzene calculated using CASSCF(7,6)/cc-pVDZ. The D_{6h} geometry was obtained at the B3LYP/6-31+G(d) level, while the C_2 geometry was taken from Bazante et al.[59] B_{2g} states are shown in red to highlight which states can mix. In both geometries, zero is set to the lowest energy state. The symmetry labels used are D_{6h} and D_{2h}.

symmetry, while B_{2g} is much higher in energy (last state in that diagram). As discussed above, in D_{2h} symmetry, E_{1g} splits and gives the B_{2g} components which can mix with the B_{2g} shape resonance.

In this work, we examine the $^2B_{2g}$ shape and core-excited resonances in benzene using single- and multireference methods and explore the mixing of the aforementioned resonant channels. Although this is not the main focus of this work, we have also calculated the lowest $^2E_{2u}$ resonance, and the results are shown in the Supporting Information.

EOM-EA-CCSD Results. The stabilization curve for the shape resonance at the EOM-EA-CCSD level is shown in Figure 7. After applying analytic continuation, the coupled-cluster calculations yield the position of the $^2B_{2g}$ shape resonance at 5.9 eV at cc-pVTZ+[p] basis set, as shown in Table 4. The energy of the shape resonance for different expansions of the GPA remains constant with a small deviation of up to 0.1 eV. The widths, however, exhibit significant change as we go from (3,3,3) and (4,4,4) to (5,5,5), where the width at (5,5,5) is 1.2 eV, while the one obtained from the former expansions is 0.7 eV.

The $^2E_{1g}$ core-excited shape resonance was obtained using EOM-EA-CCSD starting from a triplet reference. This resonance is predicted to be above the shape resonance by about 1.2−1.3 eV. From Figure 7b, we see that the two avoided crossings (first at $\alpha = 0.39$ and the second at $\alpha = 0.65$) define the core-excited resonance state. The analytic continuation results for the two avoided crossings are summarized in Table 4. The first avoided crossing provides a position of 7.23 eV and a width of 0.117 eV, which is consistent across all expansions of the GPA because of the well-defined nature of the crossing accompanied by a smaller width. The second avoided crossing reveals the resonance position at 7.31 eV with a width of 0.039 eV. Some inconsistency between the results of avoided crossings has been observed before,[23] and we believe it is because of the limitations of our basis sets. From these results, it is quite evident that the lifetime of the core-excited shape resonance is significantly higher than that of the corresponding shape of the same symmetry. The width for the core-excited state is about an order of magnitude smaller than that of the shape resonance. On the other hand, the width of the core-excited resonance here is much larger than the width in the Feshbach

https://dx.doi.org/10.1021/acs.jpca.0c07904
J. Phys. Chem. A XXXX, XXX, XXX−XXX

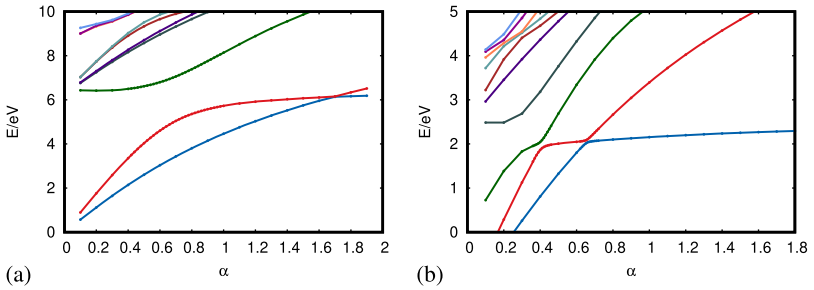

Figure 7. Stabilization curves of (a) $^2B_{2g}$ shape resonance and (b) $^2E_{1g}$ core-excited resonance in benzene at EOM-EA-CCSD/cc-pVTZ+[p] level of theory.

Table 4. Resonance Positions and Widths in eV for Benzene $^2B_{2g}$ Shape and $^2E_{1g}$ Core-Excited Resonances Obtained at the EOM-EA-CCSD/cc-pVTZ+[p] Level[a]

	$E_R(\Gamma)$		
	shape ($^2B_{2g}$)	core-excited ($^2E_{1g}$)	
GPA		AC1	AC2
(3,3,3)	5.94 (0.678)	7.23 (0.117)	7.32 (0.039)
(4,4,4)	6.02 (0.722)	7.23 (0.113)	7.31 (0.039)
(5,5,5)	5.91 (1.227)	7.23 (0.117)	7.31 (0.039)

[a]The energies are reported with respect to the neutral reference state. The core-excited resonance stabilization curve has two avoided crossings (AC1 and AC2) that are analyzed.

resonance in water. This is expected since the core-excited resonance is about 2 eV above its parent triplet state, while in water, it is below its parent neutral triplet state. Though EOM-EA-CCSD provides us with very good estimates for the energy of the resonances and their relative stability with respect to their parent neutral states, it does not provide us with any information regarding the mixing between different resonant channels. To delve into the information regarding the resonant channel mixing, we turn over to multireference methods.

Multireference Results. We performed stabilization calculations using RASSCF at the same basis set we used in EOM-EA-CCSD to determine the resonance parameters and extract information regarding the mixing. Here, both the shape and core-excited resonances are obtained from the same stabilization curves, where all states have B_{2g} symmetry in the D_{2h} point group. The stabilization curves are reported in Figure 8 and the analytic continuation results are summarized in Table 5. The position of the resonance is predicted to be at 7.5 eV, while the width is between 0.3 and 0.4 eV depending on the GPA expansion. The position of the shape resonance is overestimated by ≈1.5 eV compared to the position obtained at the EOM-EA-CCSD level, while the width is underestimated. The

Table 5. Resonance Position and Widths in eV for Benzene Shape and Core-Excited Resonances Obtained from RASSCF/cc-pVTZ+[p] and MR-CISD/cc-pVTZ+[p] Levels of Theory

	$E_R(\Gamma)$		
GPA	shape ($^2B_{2g}$)	core-excited A ($^2E_{1g}$)	core-excited B ($^2E_{1g}$)
		RASSCF	
(3,3,3)	N/A	8.26 (0.016)	9.05 (0.049)
(4,4,4)	7.54 (0.325)	8.26 (0.005)	9.05 (0.053)
(5,5,5)	7.48 (0.457)	8.26 (0.017)	9.05 (0.053)
		MR-CISD	
(3,3,3)	N/A	7.37 (0.003)	8.07 (0.023)
(4,4,4)	6.11 (0.743)	7.37 (0.003)	8.08 (0.024)
(5,5,5)	5.86 (0.534)	7.37 (0.001)	8.08 (0.024)

overestimation can be traced back to the absence of dynamical correlation in RAS and the basis set description.

The stabilization curve at the MR-CISD level is also shown in Figure 8. The position at the MR-CISD level is predicted to be 5.9−6.1 eV, comparable with that of EOM-EA-CCSD, which demonstrates the importance of adding dynamical correlation in the characterization of resonant states. The width at (5,5,5) GPA obtained from MR-CISD calculations is similar to the one obtained with (4,4,4) at the EOM-EA-CCSD level, but it is less than half of the width obtained at GPA (5,5,5) with EOM-EA-CCSD.

The resonance parameters for the core-excited resonances are reported in Table 5. We see two configurations for the core-excited shape resonances as the electrons can be paired in one of the two-fold degenerate LUMO orbitals in benzene. These correspond to one component of the energetically lowest two degenerate E_{1g} resonances. The two core-excited states captured in these calculations are separated by 0.7−0.8 eV. Overall, the resonance positions for all the three states that we located have come down by 1 eV in comparison with RAS,

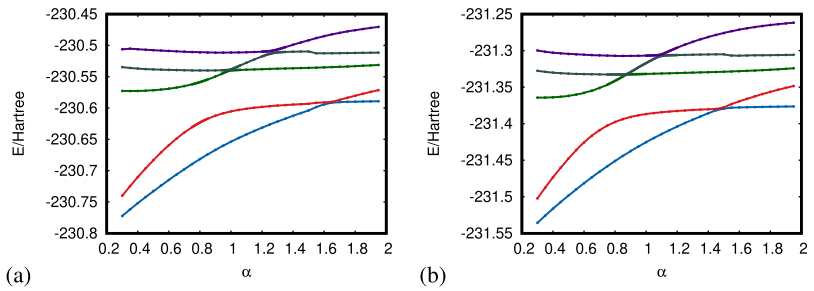

Figure 8. Stabilization curves of benzene resonances at (a) RASSCF/cc-pVTZ+[p] and (b) MR-CISD/cc-pVTZ+[p] levels.

https://dx.doi.org/10.1021/acs.jpca.0c07904
J. Phys. Chem. A XXXX, XXX, XXX−XXX

a consequence of the treatment of dynamic correlation in MR-CISD. The widths for the first 2p-1h resonance are smaller than the second according to both RASSCF and MR-CISD results, sometimes by almost an order of magnitude. For both resonances, longer lifetimes of these states are predicted compared to the shape resonance. The widths are smaller at the MR-CISD level compared to RASSCF, while the EOM-EA-CCSD width is larger than that predicted from both of the multireference methods.

In order to examine the mixing between shape and core-excited configurations, we examine the configuration interaction (CI) coefficients. At α = 1.95, we see that the CI coefficient of the shape resonant configuration is 0.65, an indication of its mixed character. The low CI coefficient indicates that there is some mixing going on with other states, and hence, this resonance is not of a pure shape character. The orbital occupation numbers for the π^* orbitals also point to that. These are as follows: 0.4 for the degenerate e_{2u} pair and 0.6 for the b_{2g} orbital. Since the configuration of the pure shape resonance should not have any occupation in the e_{2u} orbitals, these occupations are another strong evidence of heavy mixing between the b_{2g} shape and core-excited shape resonances. In D_{6h}, the immediate core-excited resonances have a different symmetry, but when the symmetry is broken, the mixing can be amplified. In order to confirm this, we also look at the CI coefficients from the small CASSCF calculations we performed using the minimum C_2 geometry. These coefficients show that at the lower symmetry, the shape resonance again has a CI coefficient around 0.65 and a coefficient of 0.58 for the $(HOMO)^1(LUMO)^2$ configuration (HOMO = highest occupied molecular orbital). It is expected that the vibrations of the molecule will break the symmetry and the mixing will be substantial. This mixing explains the observed population of the low-lying triplet excited states following the decay of the shape resonance. This study highlights the crucial role of multireference methods in providing a detailed understanding of the mixing of various resonant channels and their origin.

Comparison with Previous Results. Table 6 shows the previous results on the benzene resonances. Electron transmission spectroscopy studies by Nenner and Schulz[69] indicated that the lowest resonance in benzene was a degenerate $^2E_{2u}$ state at an energy of 1.14 eV. The same study reported that the next higher-lying resonance, which is commonly referred to as the "third" shape resonance in benzene ($^2B_{2g}$), was located at an energy of 4.85 eV. They proposed that this "third" shape resonance might be mixing with a core-excited resonance of the same symmetry because of low-lying triplet and singlet excited states in the vicinity of the resonant state. It was shown that the $^2B_{2g}$ resonance not only decays into the ground state of benzene but also to the $^3B_{1u}$, $^3E_{1u}$, and $^1B_{2u}$ excited states.[65,66] Previous theoretical study by Gianturco and Lucchese using scattering theory placed the position of the $^2B_{2g}$ resonance at 7.44 eV.[71] Bettega et al. employed Schwinger multichannel method to calculate the total electronic scattering cross sections, and they observed the position of $^2B_{2g}$ resonance at 9.4 eV within the static exchange approximation which moved to a value of 8.3 eV when polarization was included.[72] The large discrepancy in the theoretical values when compared to the experimental one is attributed to a poor description of the core-excited character in the $(N + 1)$-electron configuration space used by the authors. This discrepancy was later addressed in the work by Winstead and McKoy on the resonances of pyrazine.[74] By including triplet-coupled excitations into the description of the $(N + 1)$ electronic configuration space to treat polarization effects, the authors saw a substantial lowering of the third resonance position in pyrazine by ≈1.6 eV.[75] This observation dictates that a multiconfigurational treatment of the $(N + 1)$-electronic configuration is required for the accurate description of the "third" shape resonance in benzene and similar molecular systems. Recent works which have employed the Schwinger multichannel method with pseudo-potentials have reported an improved position for the $^2B_{2g}$ resonance at 4.9 eV with a width of 0.56 eV, the position being in excellent agreement with the experiment.[73,76] OSM using EOM-EA-CCSD on the other hand gave a value of 5.9 eV and a width of 1.4 eV.[59] Another orbital stabilization study using density functional theory gave similar positions.[70] CAP-based EOM-EA-CCSD study by Jagau and Krylov[24] reported a position of 6.75 eV for the B_{2g} shape resonance which is overestimated compared to the experiment, previous work, and current study. Jagau et al. attributed the discrepancy in their results to stabilization of a pseudo-continuum state rather than the actual resonant state due to deficiencies in the basis set size and improper choice of the CAP onset. This points to an additional problem with the CAP approach, which is the need for very large basis sets. The demands of basis sets are higher for CAP compared to the stabilization method. Even though we also do not include a very large basis set, we still obtain more accurate results than Jagau et al. with OSM.

Our results for the position of the shape $^2B_{2g}$ resonance at the EOM-EA-CCSD and MR-CISD levels are in good agreement with the previous study at the EOM-EA-CCSD level,[59] even though we used smaller basis sets. They are however still 1 eV off when compared to the experiment, where most studies predict the position of the shape resonance to be around 4.8 eV. Including correlation beyond single and double excitations and increasing the basis set size should be able to address this discrepancy. Although we did not test the effect of increasing the size of the basis set, there is some information in the literature. In an orbital stabilization study (with EOM-EA-CCSD) conducted by Falcetta et al.,[22] it was shown that the shape resonance of N_2 was only affected by 0.1 eV in the position and 0.03 eV in the width when going from aug-cc-pVTZ to aug-cc-pVQZ basis. The role of basis functions was also examined in the study by Zuev et al.[77] using CAP and EOM-EA-CCSD. It was once again observed that going from

Table 6. Selected Previous Experimental and Theoretical Studies on the Resonances in Benzene Anion[a]

	$E_R(\Gamma)$ shape ($^2B_{2g}$)	E_R core-excited ($^2E_{1g}$)
Nenner and Schulz[69] (exp)	4.85	
Allan[66] (exp)	4.8	6.5
Burrow et al.[67] (exp)	4.82	5.7, 7.5
Cheng and Shih[70] (theory)	5.5−5.9	
Gianturco and Lucchese[71] (theory)	7.44	
Bettega et al.[72] (theory)	8.3	
Bazante et al.[59] (theory)	5.93 (1.4)	
Costa et al.[73] (exp)	4.6 ± 0.2	
Costa et al.[73] (theory)	4.9 (0.56)	
Jagau and Krylov[24] (theory)	6.75 (0.35)	

[a]Positions in eV are given. The values in the brackets indicate the width of the resonance in eV.

https://dx.doi.org/10.1021/acs.jpca.0c07904
J. Phys. Chem. A XXXX, XXX, XXX−XXX

triple zeta to quadruple zeta, the resonance position changes by about 0.1 eV. Adding extra diffuse functions had a larger effect, reaching ≈0.5 eV changes in the position. Furthermore, the resonant positions obtained at the multireference level are subject to uncertainties as we saw in the case of water.

There is no experimental information on the width, and previous theoretical values have large variations. Bazante et al.[59] predicted a width of 1.4 eV using OSM, and Jagau and Krylov[24] report a width of 0.35 eV using CAP-EOM-EA-CCSD, while the scattering theory gave a value of 0.56 eV.[73] Our values also span this range, although the MR-CISD values are closer to the smaller value. In our previous study, we had reported that it is difficult to do analytic continuation of resonances with large widths.[23] It should also be expected that the mixing of the shape resonance with the core-excited ones will affect the width, most likely toward smaller values. This may be the reason that the multireference methods predict smaller widths, and this indicates that they may be more accurate.

Much more limited information exists on the core-excited resonances. Evidence for 2p-1h resonances around 6−7.5 eV have been seen in previous experiments, but there is hardly any theoretical information available. Our results are in that range. More importantly, both EOM-EA-CCSD and MR-CISD predict the first $^2E_{1g}$ resonance to be around 7.3 eV and be long-lived.

CONCLUSIONS

Two-particle one-hole resonances were investigated using OSM in combination with multireference methods and EOM-EA-CCSD when possible. In benzene, the resonances were calculated using both EOM-EA-CCSD and multireference methods. Comparing the results, we see that the resonance positions obtained from the EOM-EA-CCSD methods are in good agreement with the ones obtained from multireference calculations with dynamical correlation (MR-CISD). On the other hand, RASSCF, which lacks dynamical correlation, has significant differences compared to these methods. This demonstrates the importance of dynamical correlation in the relative energies of the resonant states. The widths of the resonances are harder to describe accurately, and they are especially challenging for broad resonances and when mixing is involved.

In order to be able to use EOM-EA-CCSD methodology to treat two-particle one-hole resonances, we need to use an appropriate triplet state as the reference. In most cases, this will give one core-excited resonance, obtained by attaching an electron to the ground triplet state obtained at CCSD. If the description of the underlying triplet reference obtained at CCSD is not parent to the resonance of interest, as we have seen in the case of water, or if we are interested in several core-excited resonances, then we are unable to use this approach. Another drawback of EOM-EA-CCSD method stems from the absence of a multiconfigurational nature of the computed excited states because of which it is difficult to obtain any information regarding the mixing of resonant channels, as in the case of benzene. A major advantage of EOM-EA-CCSD however is the accurate balance between neutral and anionic states, without the variables present in multireference methods.

On the other hand, with multireference methods, we can compute both shape and core-excited resonances in the same calculation and obtain the mixing between them, if any. One drawback of the multireference approach is the uncertainties in the calculated positions with respect to the energy of the neutral ground state. The energy of the reference ground state changes significantly upon state-averaging, which can affect the final reported positions significantly. RASSCF was found to be very sensitive, while adding dynamical correlation improves the error.

ASSOCIATED CONTENT

Supporting Information

The Supporting Information is available free of charge at https://pubs.acs.org/doi/10.1021/acs.jpca.0c07904.

Optimized coordinates of the geometries of neutral benzene and water, ACT employed in multireference calculations for both systems, and $^2E_{2u}$ resonance in benzene (PDF)

AUTHOR INFORMATION

Corresponding Author

Spiridoula Matsika − *Department of Chemistry, Temple University, Philadelphia, Pennsylvania 19122, United States;* orcid.org/0000-0003-2773-3979; Email: smatsika@temple.edu

Authors

Mushir Thodika − *Department of Chemistry, Temple University, Philadelphia, Pennsylvania 19122, United States*

Nathan Mackouse − *Department of Chemistry, Temple University, Philadelphia, Pennsylvania 19122, United States*

Complete contact information is available at: https://pubs.acs.org/10.1021/acs.jpca.0c07904

Notes

The authors declare no competing financial interest.

ACKNOWLEDGMENTS

The authors acknowledge support by the National Science Foundation under grant CHE-1800171.

REFERENCES

(1) Mason, N. J.; Nair, B.; Jheeta, S.; Szymańska, E. Electron induced chemistry: a new frontier in astrochemistry. *Faraday Discuss.* **2014**, *168*, 235−247.

(2) Boyer, M. C.; Rivas, N.; Tran, A. A.; Verish, C. A.; Arumainayagam, C. R. The role of low-energy (≤ 20 eV) electrons in astrochemistry. *Surf. Sci.* **2016**, *652*, 26−32.

(3) Bass, A. D.; Sanche, L. Dissociative electron attachment and charge transfer in condensed matter. *Radiat. Phys. Chem.* **2003**, *68*, 3−13.

(4) Arumainayagam, C. R.; Lee, H.-L.; Nelson, R. B.; Haines, D. R.; Gunawardane, R. P. Low-energy electron-induced reactions in condensed matter. *Surf. Sci. Rep.* **2010**, *65*, 1−44.

(5) Boudaïffa, B.; Cloutier, P.; Hunting, D.; Huels, M. A.; Sanche, L. Resonant formation of DNA strand breaks by low-energy (3 to 20 eV) electrons. *Science* **2000**, *287*, 1658−1660.

(6) Tonzani, S.; Greene, C. H. Low-energy electron scattering from DNA and RNA bases: Shape resonances and radiation damage. *J. Chem. Phys.* **2006**, *124*, 054312.

(7) Li, Z.; Cloutier, P.; Sanche, L.; Wagner, J. R. Low-energy electron-induced DNA damage: Effect of base sequence in oligonucleotide trimers. *J. Am. Chem. Soc.* **2010**, *132*, 5422−5427.

(8) Bald, I.; Langer, J.; Tegeder, P.; Ingólfsson, O. From isolated molecules through clusters and condensates to the building blocks of life. *Int. J. Mass Spectrom.* **2008**, *277*, 4−25.

(9) Herbert, J. M. The quantum chemistry of loosely bound electrons. *Rev. Comput. Chem.* **2015**, *28*, 391−517.
(10) Klaiman, S.; Gilary, I. *Advances in Quantum Chemistry*; Elsevier, 2012; Vol. *63*; pp 1−31.
(11) Moiseyev, N.; Certain, P. R.; Weinhold, F. Resonance properties of complex-rotated hamiltonians. *Mol. Phys.* **1978**, *36*, 1613−1630.
(12) Moiseyev, N. Quantum theory of resonances: calculating energies, widths and cross-sections by complex scaling. *Phys. Rep.* **1998**, *302*, 212−293.
(13) Simons, J. Theoretical study of negative molecular ions. *Annu. Rev. Phys. Chem.* **2011**, *62*, 107−128.
(14) Jagau, T.-C.; Bravaya, K. B.; Krylov, A. I. Extending quantum chemistry of bound states to electronic resonances. *Annu. Rev. Phys. Chem.* **2017**, *68*, 525−553.
(15) Ryaboy, V.; Moiseyev, N.; Mandelshtam, V. A.; Taylor, H. S. Resonance positions and widths by complex scaling and modified stabilization methods: van der Waals complex NeICl. *J. Chem. Phys.* **1994**, *101*, 5677−5682.
(16) Thompson, T. C.; Truhlar, D. G. Stabilization calculations of resonance energies for chemical reactions. *J. Chem. Phys.* **1982**, *76*, 1790−1794.
(17) Fennimore, M. A.; Matsika, S. Electronic Resonances of Nucleobases Using Stabilization Methods. *J. Phys. Chem. A* **2018**, *122*, 4048−4057.
(18) McCurdy, C. W.; Martín, F. Implementation of exterior complex scaling in B-splines to solve atomic and molecular collision problems. *J. Phys. B: At., Mol. Opt. Phys.* **2004**, *37*, 917.
(19) Elander, N.; Yarevsky, E. Exterior complex scaling method applied to doubly excited states of helium. *Phys. Rev. A: At., Mol., Opt. Phys.* **1998**, *57*, 3119.
(20) McCurdy, C. W., Jr.; Rescigno, T. N. Extension of the method of complex basis functions to molecular resonances. *Phys. Rev. Lett.* **1978**, *41*, 1364.
(21) Chao, J. S. Y.; Falcetta, M. F.; Jordan, K. D. Application of the stabilization method to the N_2^- ($1^2\Pi_g$) and $Mg^-(1^2P)$ temporary anion states. *J. Chem. Phys.* **1990**, *93*, 1125−1135.
(22) Falcetta, M. F.; DiFalco, L. A.; Ackerman, D. S.; Barlow, J. C.; Jordan, K. D. Assessment of various electronic structure methods for characterizing temporary anion states: Application to the ground state anions of N_2, C_2H_2, C_2H_4, and C_6H_6. *J. Phys. Chem. A* **2014**, *118*, 7489−7497.
(23) Thodika, M.; Fennimore, M.; Karsili, T. N. V.; Matsika, S. Comparative study of methodologies for calculating metastable states of small to medium-sized molecules. *J. Chem. Phys.* **2019**, *151*, 244104.
(24) Jagau, T.-C.; Krylov, A. I. Characterizing metastable states beyond energies and lifetimes: Dyson orbitals and transition dipole moments. *J. Chem. Phys.* **2016**, *144*, 054113.
(25) Benda, Z.; Jagau, T.-C. Communication: Analytic gradients for the complex absorbing potential equation-of-motion coupled-cluster method. *J. Chem. Phys.* **2017**, *146*, 031101.
(26) Benda, Z.; Jagau, T.-C. Locating Exceptional Points on Multidimensional Complex-Valued Potential Energy Surfaces. *J. Phys. Chem. Lett.* **2018**, *9*, 6978−6984.
(27) Benda, Z.; Rickmeyer, K.; Jagau, T.-C. Structure Optimization of Temporary Anions. *J. Chem. Theory Comput.* **2018**, *14*, 3468−3478.
(28) Benda, Z.; Jagau, T.-C. Understanding Processes Following Resonant Electron Attachment: Minimum-Energy Crossing Points between Anionic and Neutral Potential Energy Surfaces. *J. Chem. Theory Comput.* **2018**, *14*, 4216−4223.
(29) Bhattacharya, D.; Ben-Asher, A.; Haritan, I.; Pawlak, M.; Landau, A.; Moiseyev, N. Polyatomic ab initio complex potential energy surfaces: Illustration of ultracold collisions. *J. Chem. Theory Comput.* **2017**, *13*, 1682−1690.
(30) Landau, A.; Ben-Asher, A.; Gokhberg, K.; Cederbaum, L. S.; Moiseyev, N. Ab initio complex potential energy curves of the He*(1s2p ^{1}P)−Li dimer. *J. Chem. Phys.* **2020**, *152*, 184303.
(31) Bhattacharya, D.; Landau, A.; Moiseyev, N. Ab Initio Complex Transition Dipoles between Autoionizing Resonance States from Real Stabilization Graphs. *J. Phys. Chem. Lett.* **2020**, *11*, 5601−5609.
(32) Hazi, A. U.; Taylor, H. S. Stabilization method of calculating resonance energies: model problem. *Phys. Rev. A: At., Mol., Opt. Phys.* **1970**, *1*, 1109.
(33) Taylor, H. S. Models, interpretations, and calculations concerning resonant electron scattering processes in atoms and molecules. *Adv. Chem. Phys.* **1970**, *18*, 91−147.
(34) Simons, J. Resonance state lifetimes from stabilization graphs. *J. Chem. Phys.* **1981**, *75*, 2465−2467.
(35) Jordan, K. D. Padé approximants: An alternative analytic representation of the potential curves for diatomic molecules. *J. Mol. Spectrosc.* **1975**, *56*, 329−331.
(36) Yu, L.; Chao, J. S.-Y. Application of Analytic Continuations to Avoided Crossings. *J. Chin. Chem. Soc.* **1993**, *40*, 11−22.
(37) Dunning, T. H., Jr. Gaussian basis sets for use in correlated molecular calculations. I. The atoms boron through neon and hydrogen. *J. Chem. Phys.* **1989**, *90*, 1007−1023.
(38) Stanton, J. F.; Bartlett, R. J. The equation of motion coupled-cluster method. A systematic biorthogonal approach to molecular excitation energies, transition probabilities, and excited state properties. *J. Chem. Phys.* **1993**, *98*, 7029−7039.
(39) Stanton, J. F.; Gauss, J. Analytic energy derivatives for ionized states described by the equation-of-motion coupled cluster method. *J. Chem. Phys.* **1994**, *101*, 8938−8944.
(40) Nooijen, M.; Bartlett, R. J. Equation of motion coupled cluster method for electron attachment. *J. Chem. Phys.* **1995**, *102*, 3629−3647.
(41) Krylov, A. I. Equation-of-motion coupled-cluster methods for open-shell and electronically excited species: The hitchhiker's guide to Fock space. *Annu. Rev. Phys. Chem.* **2008**, *59*, 433−462.
(42) Werner, H.-J. Matrix-formulated direct multiconfiguration self-consistent field and multiconfiguration reference configuration-interaction methods. *Adv. Chem. Phys.* **1987**, *69*, 1−62.
(43) Frisch, M.; Trucks, G.; Schlegel, H.; Scuseria, G.; Robb, M.; Cheeseman, J.; Scalmani, G.; Barone, V.; Mennucci, B.; Petersson, G.; et al. *Gaussian 09 Program*; Gaussian Inc.: Wallingford, CT, 2009.
(44) Werner, H.-J.; Knowles, P. J.; Knizia, G.; Manby, F. R.; Schütz, M. Molpro: a general-purpose quantum chemistry program package. *Wiley Interdiscip. Rev.: Comput. Mol. Sci.* **2012**, *2*, 242−253.
(45) Shao, Y.; Gan, Z.; Epifanovsky, E.; Gilbert, A. T.; Wormit, M.; Kussmann, J.; Lange, A. W.; Behn, A.; Deng, J.; Feng, X.; et al. Advances in molecular quantum chemistry contained in the Q-Chem 4 program package. *Mol. Phys.* **2015**, *113*, 184−215.
(46) Rubio, M.; Serrano-Andrés, L.; Merchán, M. Excited states of the water molecule: Analysis of the valence and Rydberg character. *J. Chem. Phys.* **2008**, *128*, 104305.
(47) Mulliken, R. S. Rydberg states and Rydbergization. *Acc. Chem. Res.* **1976**, *9*, 7−12.
(48) Lozier, W. W. Negative ions in hydrogen and water vapor. *Phys. Rev.* **1930**, *36*, 1417.
(49) Mann, M. M.; Hustrulid, A.; Tate, J. T. The ionization and dissociation of water vapor and ammonia by electron impact. *Phys. Rev.* **1940**, *58*, 340.
(50) Schulz, G. J. Excitation and negative ions in H2O. *J. Chem. Phys.* **1960**, *33*, 1661−1665.
(51) Compton, R. N.; Christophorou, L. G. Negative-Ion Formation in H2O and D2O. *Phys. Rev.* **1967**, *154*, 110.
(52) Gorfinkiel, J. D.; Morgan, L. A.; Tennyson, J. Electron impact dissociative excitation of water within the adiabatic nuclei approximation. *J. Phys. B: At., Mol. Opt. Phys.* **2002**, *35*, 543.
(53) Haxton, D. J.; Zhang, Z.; McCurdy, C. W.; Rescigno, T. N. Complex potential surface for the B 1 2 metastable state of the water anion. *Phys. Rev. A: At., Mol., Opt. Phys.* **2004**, *69*, 062713.
(54) Haxton, D. J.; McCurdy, C. W.; Rescigno, T. N. Dissociative electron attachment to the H 2 O molecule I. Complex-valued potential-energy surfaces for the B 1 2, A 1 2, and B 2 2 metastable

https://dx.doi.org/10.1021/acs.jpca.0c07904
J. Phys. Chem. A XXXX, XXX, XXX−XXX

states of the water anion. *Phys. Rev. A: At., Mol., Opt. Phys.* **2007**, *75*, 012710.
(55) Buchelnikova, I. Cross Sections for the Capture of Slow Electrons by O_2 and H_2O Molecules and Molecules of Halogen Compounds (English translation). *Soviet Physics - JETP* **1959**, *35*, 783−791.
(56) Trajmar, S.; Hall, R. I. Dissociative electron attachment H_2O and D_2O - energy and angular distribution of H^- and D^- fragments. *J. Phys. B: At., Mol. Opt. Phys.* **1974**, *7*, L458−L461.
(57) Jungen, M.; Vogt, J.; Staemmler, V. Feshbach-resonances and dissociative electron attachment of H_2O. *Chem. Phys.* **1979**, *37*, 49−55.
(58) Belic, D. S.; Landau, M.; Hall, R. I. Energy and angular dependence of H-(D-) ions produced by dissociative electron attachment to H2O (D2O). *J. Phys. B: At., Mol. Opt. Phys.* **1981**, *14*, 175.
(59) Bazante, A. P.; Davidson, E. R.; Bartlett, R. J. The benzene radical anion: A computationally demanding prototype for aromatic anions. *J. Chem. Phys.* **2015**, *142*, 204304.
(60) Christiansen, O.; Koch, H.; Halkier, A.; Jo/rgensen, P.; Helgaker, T.; Sánchez de Merás, A. Large-scale calculations of excitation energies in coupled cluster theory: The singlet excited states of benzene. *J. Chem. Phys.* **1996**, *105*, 6921−6939.
(61) Hald, K.; Jørgensen, P.; Christiansen, O.; Koch, H. Implementation of electronic ground states and singlet and triplet excitation energies in coupled cluster theory with approximate triples corrections. *J. Chem. Phys.* **2002**, *116*, 5963−5970.
(62) Schreiber, M.; Silva-Junior, M. R.; Sauer, S. P. A.; Thiel, W. Benchmarks for electronically excited states: CASPT2, CC2, CCSD, and CC3. *J. Chem. Phys.* **2008**, *128*, 134110.
(63) Silva-Junior, M. R.; Schreiber, M.; Sauer, S. P. A.; Thiel, W. Benchmarks of electronically excited states: Basis set effects on CASPT2 results. *J. Chem. Phys.* **2010**, *133*, 174318.
(64) Loos, P.-F.; Lipparini, F.; Boggio-Pasqua, M.; Scemama, A.; Jacquemin, D. A Mountaineering Strategy to Excited States: Highly Accurate Energies and Benchmarks for Medium Sized Molecules. *J. Chem. Theory Comput.* **2020**, *16*, 1711−1741.
(65) Azria, R.; Schulz, G. Vibrational and triplet excitation by electron impact in benzene. *J. Chem. Phys.* **1975**, *62*, 573−575.
(66) Allan, M. Forward electron scattering in benzene; forbidden transitions and excitation functions. *Helv. Chim. Acta* **1982**, *65*, 2008−2023.
(67) Burrow, P. D.; Michejda, J. A.; Jordan, K. D. Electron transmission study of the temporary negative ion states of selected benzenoid and conjugated aromatic hydrocarbons. *J. Chem. Phys.* **1987**, *86*, 9−24.
(68) Hobey, W. D.; McLachlan, A. D. Dynamical Jahn-Teller Effect in Hydrocarbon Radicals. *J. Chem. Phys.* **1960**, *33*, 1695−1703.
(69) Nenner, I.; Schulz, G. J. Temporary negative ions and electron affinities of benzene and N-heterocyclic molecules: pyridine, pyridazine, pyrimidine, pyrazine, and s-triazine. *J. Chem. Phys.* **1975**, *62*, 1747−1758.
(70) Cheng, H.-Y.; Shih, C.-C. Application of the Stabilization Method to the π^* Temporary Anion States of Benzene and Substituted Benzenes in Density Functional Theory. *J. Phys. Chem. A* **2009**, *113*, 1548−1554.
(71) Gianturco, F. A.; Lucchese, R. R. One-electron resonances and computed cross sections in electron scattering from the benzene molecule. *J. Chem. Phys.* **1998**, *108*, 6144−6159.
(72) Bettega, M. H. F.; Winstead, C.; McKoy, V. Elastic scattering of low-energy electrons by benzene. *J. Chem. Phys.* **2000**, *112*, 8806−8812.
(73) Costa, F.; Álvarez, L.; Lozano, A. I.; Blanco, F.; Oller, J. C.; Muñoz, A.; Barbosa, A. S.; Bettega, M. H. F.; Ferreira Da Silva, F.; Limão-Vieira, P.; et al. Experimental and theoretical analysis for total electron scattering cross sections of benzene. *J. Chem. Phys.* **2019**, *151*, 084310.
(74) Winstead, C.; McKoy, V. Low-energy electron scattering by pyrazine. *Phys. Rev. A: At., Mol., Opt. Phys.* **2007**, *76*, 012712.
(75) Winstead, C.; McKoy, V. Resonant channel coupling in electron scattering by pyrazine. *Phys. Rev. Lett.* **2007**, *98*, 113201.
(76) Barbosa, A. S.; Bettega, M. H. F. Shape resonances, virtual state, and Ramsauer-Townsend minimum in the low-energy electron collisions with benzene. *J. Chem. Phys.* **2017**, *146*, 154302.
(77) Zuev, D.; Jagau, T.-C.; Bravaya, K. B.; Epifanovsky, E.; Shao, Y.; Sundstrom, E.; Head-Gordon, M.; Krylov, A. I. Complex absorbing potentials within EOM-CC family of methods: Theory, implementation, and benchmarks. *J. Chem. Phys.* **2014**, *141*, 024102.

https://dx.doi.org/10.1021/acs.jpca.0c07904
J. Phys. Chem. A XXXX, XXX, XXX−XXX